

**IMMOBILISATION OF TiO₂ POWDER ONTO
GLASS PLATES VIA DIP-COATING
TECHNIQUE USING ENR-50/PVC POLYMER
BLEND AS ADHESIVES AND ITS
PHOTOCATALYTIC APPLICATION**

NGOH YING SHIN

UNIVERSITI SAINS MALAYSIA

2010

IMMOBILISATION OF TiO₂ POWDER ONTO GLASS PLATES VIA DIP-COATING TECHNIQUE USING ENR-50/PVC POLYMER BLEND AS ADHESIVES AND ITS PHOTOCATALYTIC APPLICATION

by

NGOH YING SHIN

**Thesis submitted in fulfilment of the requirements for the degree of
Master of Science**

April 2010

ACKNOWLEDGEMENTS

Hereby, I would like to convey my utmost appreciation to those who has assisted me one way or the other in making this research and thesis a reality. First of all, I am deeply indebted to my research supervisor, Professor Dr. Mohd. Asri Mohd. Nawi for giving me the opportunity to pursue this interesting research. I would like to take this chance to sincerely thank Professor for his endless guidance, invaluable advice and patience throughout my candidature.

I would also like to extend my gratitude to the Malaysia's Ministry of Science and Technology for funding this research under FRGS: 203/227/PKIMIA/67/027 and IRPA: 305/229/PKIMIA/613402. I am earnestly grateful to Universiti Sains Malaysia (USM) for the scholarship under USM Fellowship Scheme. Also on this list are the staffs from School of Chemical Sciences, School of Biological Sciences and Institute of Postgraduate Studies USM for their dedications and contributions in their respective expertises. I would also like to thank Professor Dr. Jamil Ismail for the use of the particle analysis software. My special thanks go out to all members of Photocatalysis Laboratory for their co-operations and inspirations during the course of this research. I would also like to express my gratitude to all my friends for their encouragement and supports.

Last but not least, I would like to extend my most heartfelt appreciation to my parents and sister for their continuous moral support and most importantly, their belief in me during trying and challenging times. This research has been a wonderful learning journey and I thank each and every one of you for making it happened!

NGOH YING SHIN

TABLE OF CONTENTS

	Page
ACKNOWLEDGEMENTS	ii
TABLE OF CONTENTS	iii
LIST OF TABLES	ix
LIST OF FIGURES	xi
LIST OF PLATES	xv
LIST OF ABBREVIATIONS	xvi
ABSTRAK	xvii
ABSTRACT	xix
CHAPTER 1	INTRODUCTION AND LITERATURE REVIEWS
1.0	General 1
1.1	Advanced Oxidation Processes (AOPs) 3
1.1.1	Processes of AOPs 5
1.1.2	Environmental applications of AOPs 7
1.2	Heterogeneous photocatalysis 10
1.2.1	Overview 10
1.2.2	Background 11
1.2.3	Semiconductor mediated heterogeneous photocatalysis 12
1.3	Titanium dioxide (TiO ₂) 15
1.3.1	General 15
1.3.2	Crystal structures of TiO ₂ 18
1.4	TiO ₂ as semiconductor photocatalyst 20

1.5	General mechanism pathway of TiO ₂ photocatalysis	22
1.6	Langmuir-Hinshelwood process	24
1.7	Applications of TiO ₂	27
1.8	Immobilisation of TiO ₂ photocatalyst	30
1.9	Textile industry effluents	44
1.9.1	Overview	44
1.9.2	Treatment of textile effluents	45
1.9.3	Methylene blue	48
1.9.3.1	Applications of MB	50
1.9.3.2	Toxicity of MB	52
1.10	Polymer blend	53
1.10.1	Overview	53
1.10.2	Epoxidised natural rubber	55
1.10.3	Poly (vinyl) chloride (PVC)	57
1.10.4	Epoxidised natural rubber (ENR-50)/poly (vinyl) chloride (PVC) blend	61
1.11	Problem statement and research objectives	62
CHAPTER 2 MATERIALS AND METHODS		
2.0	Materials and Methods	64
2.1	Chemical and reagents	64
2.2	Instruments and equipments	64
2.3	Preparation of chemical solutions	66
2.3.1	Methylene blue (MB) solution	66
2.3.2	Epoxidised natural rubber-50 (ENR-50)	66
2.3.2.1	Determination of the ratio of ENR-50 to toluene	67

2.3.3	Preparation of COD reagent in test tubes	67
2.3.3.1	Standardization of COD reagent	68
2.4	Optimisation of ENR-50 to PVC ratio in TiO ₂ /ENR/PVC/glass plates	68
2.4.1	Preparation of TiO ₂ /ENR/PVC dip-coating formulation	68
2.4.1.1	Optimisation of PVC in TiO ₂ /ENR/PVC dip-coating formulation	68
2.4.1.2	Optimisation of ENR-50 solution in TiO ₂ /ENR/PVC coating formulation	69
2.4.2	Preparation of TiO ₂ /ENR/PVC coated glass plates	70
2.5	Photocatalytic reactor set-up	72
2.6	Photocatalytic degradation of MB	73
2.6.1	Photocatalytic degradation of MB using TiO ₂ /ENR/PVC/glass plates	73
2.6.2	Photocatalytic degradation of MB using TiO ₂ powder slurry technique	73
2.7	Adsorption study of MB	74
2.8	Adhesion of the immobilised TiO ₂ coatings onto glass plates	74
2.9	Characterisation of TiO ₂ coating	75
2.10	Optimization of operational parameters for the degradation of MB using TiO ₂ /ENR/PVC	75
2.10.1	Effect of photocatalyst loading on photocatalytic activity	75
2.10.2	Effect of pH on the photocatalytic activity of TiO ₂ /ENR/PVC/glass plates	76
2.10.2.1	Determination of point of zero charge (pH _{pzc}) for TiO ₂ /ENR/PVC	76
2.10.2.2	Effect of initial pH of MB on its photocatalytic and adsorption activity	76
2.10.3	Effect of aeration rates on photocatalytic activity	77
2.10.4	Effect of initial concentration of MB on its photocatalytic degradation	77

2.10.5	Effect of UV light intensity on the photocatalytic degradation of MB	77
2.10.5.1	UV filter	78
2.11	Reusability study of the fabricated photocatalyst plates	78
2.11.1	Sustainability in photocatalytic efficiency	78
2.11.2	Effect of interval cleaning for the TiO ₂ /ENR/PVC/glass plates during reusability test	79
2.12	Degradation of polymers within the TiO ₂ /ENR/PVC/glass plates	79
2.12.1	Durability of ENR-50/PVC polymer blend during repeated applications	79
2.12.1.1	COD testing	79
2.12.1.2	SEM-EDX analysis	80
2.12.1.3	TGA analysis	80
2.12.1.4	FTIR analysis	81
2.13	Mineralization of MB	81
2.13.1	COD testing	81
2.13.2	MB colour removal	82
2.13.3	Monitoring pH changes of MB solution	82
2.13.4	Detection of inorganic compounds (SO ₄ ²⁻ , NO ₃ ⁻ , Cl ⁻) using ion chromatography	82
2.13.4.1	Set-up procedures for ion chromatography	82
2.13.4.2	Detection of anions (SO ₄ ²⁻ , NO ₃ ⁻ , Cl ⁻)	83
 CHAPTER 3 RESULTS AND DISCUSSIONS		
3.0	Results and discussions	84
3.1	Fabrication of TiO ₂ /ENR/PVC/glass system	84
3.1.1	Preparation of the dip-coating formulation	88

3.1.1.1	Optimisation of the amount of PVC powder in TiO ₂ /ENR/PVC dip-coating formulation	88
3.1.1.2	Optimisation of the amount of ENR-50 in TiO ₂ /ENR/PVC coating formulation	95
3.1.2	Coating adherence	100
3.1.2.1	Effect of amount of PVC powder on the coating adherence	100
3.1.2.2	Effect of the amount of ENR-50 on the coating adherence	103
3.2	Characterisation of the immobilised TiO ₂ photocatalyst	107
3.2.1	SEM-EDX analysis	107
3.2.2	BET analysis	111
3.2.3	FTIR	113
3.3	Photocatalytic activity comparison between immobilised TiO ₂ and TiO ₂ powder in slurry mode	115
3.4	Effect of operational parameters	120
3.4.1	Catalyst loading	120
3.4.2	Initial pH	125
3.4.3	Aeration rate	130
3.4.4	Initial dye concentration	133
3.4.5	UV irradiation	137
3.5	Reusability of the TiO ₂ /ENR/PVC/glass system	142
3.5.1	Comparison between TiO ₂ /ENR/glass and TiO ₂ /ENR/PVC/glass systems	143
3.5.2	Effect of UV irradiance	145
3.5.3	Effect of cleaning process after each cycle of photocatalytic degradation of MB	151
3.6	Evaluation of binder system under irradiation of light during repeated usages TiO ₂ /ENR/PVC/glass system	153

3.6.1	COD test	154
3.6.2	SEM-EDX analysis	159
3.6.3	TGA	163
3.6.4	FTIR analysis	171
3.7	Mineralisation of MB	174
3.7.1	COD test	175
3.7.2	Detection of inorganic compounds (H^+ , SO_4^{2-} , NO_3^- and Cl^-)	178
3.8	Effect of different support materials (glass, acrylic, PVC, PET) on the photocatalytic degradation of MB	185
CHAPTER 4 CONCLUSIONS		
4.0	Conclusions	187
CHAPTER 5 FUTURE WORKS		
5.0	Future works	192
REFERENCES		194
APPENDICES		206
LIST OF SEMINAR PRESENTATIONS		215

LIST OF TABLES

		Page
Table 1.1	Physical properties of anatase, rutile and brookite [45]	20
Table 1.2	The bands positions of some common semiconductors in aqueous solution at pH 1 [31]	21
Table 1.3	Summary of some of the immobilisation techniques for TiO ₂ photocatalyst	34
Table 1.4	Physical and chemical properties of MB [102]	50
Table 1.5	Typical applications of PVC (rigid and flexible) [113]	60
Table 3.1 (a)	Percentage of MB remaining (average) using immobilised TiO ₂ /ENR/PVC with different amount of PVC (0.00 g to 0.50g) during 90 min of photocatalytic treatment	91
Table 3.1 (b)	Percentage of MB remaining (average) using immobilised TiO ₂ /ENR/PVC with different amount of PVC (0.60 g to 1.00 g) during 90 min of photocatalytic treatment	91
Table 3.2 (a)	Percentage of MB remaining (average) using immobilised TiO ₂ /ENR/PVC with different amount of PVC (0.00g to 0.50 g) during 90 min of adsorption treatment	93
Table 3.2 (b)	Percentage of MB remaining (average) using immobilised TiO ₂ /ENR/PVC with different amount of PVC (0.60 g to 1.00 g) during 90 min of adsorption treatment	93
Table 3.3	Minimum time required for the emulsification of TiO ₂ /ENR/PVC with different amount of ENR-50 solution	96
Table 3.4	Percentage of MB remaining (average) using immobilised TiO ₂ /ENR/PVC with different amount of ENR-50 during 90 min of photocatalytic treatment	98
Table 3.5	Percentage of MB remaining (average) using immobilised TiO ₂ /ENR/PVC with different amount of ENR-50 during 90 min of adsorption treatment	98
Table 3.6	Elemental compositions of TiO ₂ powder and immobilised TiO ₂ powder	111

Table 3.7	BET surface area of TiO ₂ powder and immobilised TiO ₂ powder	113
Table 3.8	Point of zero charge for TiO ₂ anatase powder and the immobilised TiO ₂ powder	127
Table 3.9	The pseudo-first-order rate constants and their respective coefficient of determination values, R^2 , for the photocatalytic degradation of MB at different initial concentrations	136
Table 3.10	UV irradiance from different 45 W fluorescent lamps	138
Table 3.11	The loss of TiO ₂ coatings during 10 cycles of photocatalytic degradation of MB	149
Table 3.12	The reusability of the immobilised TiO ₂ /ENR/PVC in the photocatalytic degradation of MB upon 10 cycles of 90 min repeated applications under irradiation of lamps with different amount of UV irradiance	150
Table 3.13	EDX analysis of before and after used immobilised TiO ₂ /ENR/PVC	162
Table 3.14	Average particle size of the before and after used immobilised TiO ₂ /ENR/PVC	163
Table 3.15	Thermogravimetric data of ENR-50, PVC and the before and after used immobilised TiO ₂ /ENR/PVC	170

LIST OF FIGURES

		Page
Figure 1.1	Major advanced oxidative processes (AOPs) and their various systems [5]	4
Figure 1.2	Valence and conduction band positions of some of the most commonly used semiconductor photocatalyst at pH = 0 [30]	14
Figure 1.3	The representative crystals structures of (a) anatase (b) rutile and (c) brookite [48]	18
Figure 1.4	General mechanism pathway of TiO ₂ photocatalysis [54]	24
Figure 1.5	Molecular structure of methylene blue (C. I. Basic Blue 9, 52015) [98]	49
Figure 1.6	Structure of natural rubber and epoxidised natural rubber	56
Figure 1.7	Repeated unit of PVC structure	58
Figure 2.1	Dip-coating process set-up	71
Figure 2.2	Schematic diagram of photocatalytic experimental set-up	72
Figure 3.1	Pseudo-first-order rate constant for different amount of PVC in TiO ₂ /ENR/PVC formulations in the photocatalytic degradation and adsorption of 12 mg L ⁻¹ MB in aqueous solution	94
Figure 3.2	Pseudo-first-order rate constant for different amount of ENR-50 in TiO ₂ /ENR/PVC formulations in the photocatalytic degradation and adsorption of 12 mg L ⁻¹ MB in aqueous solution	99
Figure 3.3	Relative strength of immobilised TiO ₂ /ENR/PVC prepared with dip-coating formulations containing different amount of PVC powder and fixed amount of 5 g ENR-50 upon 30 s of interval sonication in 40 kHz ultra sonic cleaner	102
Figure 3.4	Relative strength of immobilised TiO ₂ /ENR/PVC prepared with dip-coating formulations containing different amount of ENR-50 and fixed amount of 0.80 g PVC powder upon 30 s of interval sonication in 40 kHz ultra sonic cleaner	105
Figure 3.5	FTIR spectra of (a) TiO ₂ powder, (b) TiO ₂ /ENR, (c) TiO ₂ /PVC and (d) TiO ₂ /ENR/PVC using KBr pellet	114

Figure 3.6	Pseudo-first-order rate constants and total percentage of degradation of 12 mg L ⁻¹ MB via photocatalysis and adsorption using TiO ₂ in aqueous slurry, TiO ₂ /ENR and TiO ₂ /ENR/PVC. Catalyst loading = 1.0 mg cm ⁻² , light source = 45 W fluorescent lamp with UV irradiance of 4.35 W m ⁻² , aeration rate = 100 mL min ⁻¹ and pH = 10	117
Figure 3.7	Percentage of MB removal for the different catalyst loading of the optimised TiO ₂ /ENR/PVC coating formulation in the photocatalytic degradation of 12 mg L ⁻¹ MB. Light source: 45 W fluorescent lamp with UV irradiance of 4.35 W m ⁻² , aeration rate = 100 mL min ⁻¹ , pH = 8	122
Figure 3.8	Pseudo-first-order rate constants for the different catalyst loading of the optimized TiO ₂ /ENR/PVC coating formulation in the photocatalytic degradation and adsorption of 12 mg L ⁻¹ MB. Light source = 45 W fluorescent lamp with UV irradiance of 4.35 W m ⁻² , aeration rate = 100 mL min ⁻¹ and pH = 8	123
Figure 3.9	Percentage of MB removal at different pH using the optimized TiO ₂ /ENR/PVC coating formulation in the photocatalytic degradation of 12 mg L ⁻¹ MB. Catalyst loading = 1.00 mg cm ⁻² , Light source: 45 W fluorescent lamp with UV irradiance of 4.35 W m ⁻² , aeration rate = 100 mL min ⁻¹	128
Figure 3.10	Pseudo-first-order rate constants for the photocatalytic degradation and adsorption of 12 mg L ⁻¹ MB in aqueous solution at different pH values. Catalyst loading = 1.0 mg cm ⁻² , light source = 45 W fluorescent lamp with UV irradiance of 4.35 W m ⁻² , aeration rate = 100 mL min ⁻¹	129
Figure 3.11	Pseudo-first-order rate constants for the photocatalytic degradation and adsorption of 12 mg L ⁻¹ MB in aqueous solution at different aeration flow rate. Catalyst loading = 1.0 mg cm ⁻² , light source = 45 W fluorescent lamp with UV irradiance of 4.35 W m ⁻² and pH = 8	131
Figure 3.12	Pseudo-first-order rate constants for the photocatalytic degradation of MB at different initial concentration. Catalyst loading = 1.0 mg cm ⁻² , light source = 45 W fluorescent lamp with UV irradiance of 4.35 W m ⁻² , aeration rate = 100 mL min ⁻¹ and pH = 8	135
Figure 3.13	Pseudo-first-order rate constants of 3 consecutive cycles of photocatalytic degradation of MB using 45 W fluorescent lamps with different UV irradiances	140

Figure 3.14	Comparisons of pseudo-first-order rate constants for the photocatalytic degradation of MB by immobilised TiO ₂ powder with two different binder systems, namely ENR-50 and polymer blend ENR-50/PVC	144
Figure 3.15	Pseudo-first-order rate constants of photocatalytic degradation of 12 mg L ⁻¹ MB up to 10 cycles of repeated applications under the irradiation of 45 W fluorescent lamp with UV irradiances of 1.67, 4.35 and 6.30 W m ⁻²	147
Figure 3.16	Pseudo-first-order rate constant for photocatalytic degradation of 12 mg L ⁻¹ MB up to 10 cycles of repeated applications under the irradiation of 45 W fluorescent lamp with UV irradiance of 4.35 W m ⁻² using intermittently cleaned and not cleaned coated glass plates	152
Figure 3.17	COD values of water sample irradiated under lamps with UV irradiances of 4.35 and 6.30 W m ⁻² in the presence of immobilised TiO ₂ /ENR/PVC over the span of 10 hours of irradiation	155
Figure 3.18	COD values of water sample irradiated under lamp with UV irradiance of 6.30 W m ⁻² in the presence of immobilised TiO ₂ /0.50 g ENR/PVC and TiO ₂ /2 g ENR/PVC over the span of 10 h	158
Figure 3.19	Thermogravimetric curve of ENR-50	164
Figure 3.20	Thermogravimetric curve of PVC powder	165
Figure 3.21	Thermogravimetric curve of the ‘as prepared’ immobilised TiO ₂ /ENR/PVC	168
Figure 3.22	Thermogravimetric curve of the immobilised TiO ₂ /ENR/PVC after one cycle of application	168
Figure 3.23	Thermogravimetric curve of the immobilised TiO ₂ /ENR/PVC after third cycle of application	169
Figure 3.24	Thermogravimetric curve of the immobilised TiO ₂ /ENR/PVC after tenth cycle of application	169
Figure 3.25	FTIR spectrum of (a) the ‘as prepared’ immobilised TiO ₂ /ENR/PVC, (b) the immobilised TiO ₂ /ENR/PVC after one application, (c) the immobilised TiO ₂ /ENR/PVC after three applications and (d) the immobilised TiO ₂ /ENR/PVC after ten applications	173

Figure 3.26	COD values and percentage of colour degradation of MB using TiO ₂ slurry, ‘uncleaned’ immobilised TiO ₂ /ENR/PVC and ‘cleaned’ immobilised TiO ₂ /ENR/PVC. Catalyst loading = 1.0 mg cm ⁻² , light source = 45 W fluorescent lamp with UV irradiance of 4.35 W m ⁻² , aeration rate 100 mL min ⁻¹ and pH = 8	177
Figure 3.27	pH changes in MB solution upon subsequent photocatalysis and adsorption study	179
Figure 3.28	Sulphate ions in MB solution treated by TiO ₂ slurry, ‘uncleaned’ immobilised TiO ₂ /ENR/PVC and ‘cleaned’ immobilised TiO ₂ /ENR/PVC under illumination of lamp with UV irradiance of 4.35 W m ⁻² . Catalyst loading = 1.0 mg cm ⁻² , pH = 8, aeration rate = 100 mL min ⁻¹ and initial MB concentration = 20 mg L ⁻¹	182
Figure 3.29	Nitrate ions in MB solution treated by TiO ₂ slurry, ‘uncleaned’ immobilised TiO ₂ /ENR/PVC and ‘cleaned’ immobilised TiO ₂ /ENR/PVC under illumination of lamp with UV irradiance of 4.35 W m ⁻² . Catalyst loading = 1.0 mg cm ⁻² , pH = 8, aeration rate = 100 mL min ⁻¹ and initial MB concentration = 20 mg L ⁻¹	183
Figure 3.30	Chloride ions in MB solution treated by TiO ₂ slurry, ‘uncleaned’ immobilised TiO ₂ /ENR/PVC and ‘cleaned’ immobilised TiO ₂ /ENR/PVC under illumination of lamp with UV irradiance of 4.35 W m ⁻² . Catalyst loading = 1.0 mg cm ⁻² , pH = 8, aeration rate = 100 mL min ⁻¹ and initial MB concentration = 20 mg L ⁻¹	184
Figure 3.31	Pseudo-first-order rate constants of the photocatalytic degradation of MB using immobilised TiO ₂ /ENR/PVC on different type of support materials	186

LIST OF PLATES

		Page
Plate 3.1	Glass plate coated with TiO ₂ emulsions via simple dip-coating technique	85
Plate 3.2	Immobilised TiO ₂ powder on (a) acrylic (b) PVC (c) Teflon (d) nylon and (e) aluminium via simple dip-coating technique	86
Plate 3.3	Glass plate coated with emulsions produced via continuous sonications at the temperature of 65 °C	89
Plate 3.4	SEM micrograph of TiO ₂ powder (99 % anatase) under 10 000 x magnification [116]	107
Plate 3.5	SEM micrograph of immobilised TiO ₂ /ENR prepared from dip-coating formulation containing 2 g of ENR-50 (12 w/w %) under 10 000 x magnification	108
Plate 3.6	SEM micrograph of immobilised TiO ₂ /ENR/PVC prepared from dip-coating formulation containing 2 g of ENR-50 (12 w/w %) and 0.80 g of PVC powder under 10 000 x magnification	108
Plate 3.7	SEM micrograph of immobilised TiO ₂ /ENR/PVC prepared from dip-coating formulation containing 2 g of ENR-50 (12 w/w %) and 1.00 g of PVC powder under 10 000 x magnification	109
Plate 3.8	The photographs of the immobilised TiO ₂ coating supported on glass plates after two repeated applications: (a) untreated (b) treated in ultra pure water under irradiation	153
Plate 3.9	SEM micrographs of TiO ₂ /ENR/PVC (a) before application, and after (b) first, (c) third and (d) tenth cycles of application under 50 000 x magnification	161

LIST OF ABBREVIATIONS

AOPs	Advanced Oxidation Processes
BET	Brunner-Emmet-Teller
COD	Chemical Oxygen Demand
e^-	Negatively charged electron
EDX	Energy dispersive x-ray
ENR-50	Epoxidised Natural Rubber (50% mol)
FTIR	Fourier transform infra red
h	hour
h^+	Positively charged hole
L-H	Langmuir-Hinshelwood
MB	Methylene Blue
min	Minute
PET	Polyethylene Terephthalate
pHpzc	pH at point of zero charge
PVC	Poly (vinyl) chloride
S	Second
SEM	Scanning Electron Microscopy
TGA	Thermogravimetric analysis
UV	Ultra violet
W	Watt

**PEMEGUNAN SERBUK TiO₂ PADA PLAT KACA MELALUI KAEDAH
PENYADURAN CELUP MENGGUNAKAN ADUNAN POLIMER ENR-
50/PVC SEBAGAI PELEKAT DAN APLIKASI
PEMFOTOMANGKINANNYA**

ABSTRAK

Kajian ini bertujuan untuk menghasilkan serbuk TiO₂ terpegun pada plat kaca yang boleh digunasemula berulang kali dengan menggunakan adunan polimer sebagai pelekat untuk penguraian pemfotomangkinan larutan akueus metilena biru (MB). Serbuk TiO₂ (99 % anatase) dipegunkan secara terus pada plat kaca menggunakan adunan polimer getah asli terepoksi (ENR-50) / poli vinil klorida (PVC) sebagai pelekat melalui kaedah penyaduran celup mudah. Kecekapan pemfotomangkinan serbuk TiO₂ yang dipegunkan pada plat kaca diuji dengan penguraian larutan akueus MB di bawah penyinaran lampu pendafluor 45 W. Nisbah optimum ENR-50 kepada PVC yang didapati adalah 1:3. Kecekapan pemfotomangkinan TiO₂/ENR/PVC yang dipegunkan pada plat kaca dalam penguraian larutan akueus MB adalah lebih baik berbanding dengan kebolehan pemfotomangkinan serbuk TiO₂ dalam mod penyebaran. Muatan mangkin yang optimum adalah sebanyak 1.0 mg cm⁻² dan kadar penguraian pemfotomangkinan MB adalah paling tinggi pada pH 12. Kehadiran aliran udara sebagai sumber oksigen meningkatkan kadar penguraian MB. Kebocoran UV daripada lampu pendafluor memainkan peranan yang penting dalam keberkesanan TiO₂ yang terpegun pada plat kaca. Kebolegunaan dan kebolehulangan aktiviti TiO₂/ENR/PVC terpegun meningkat sejajar dengan keamatan kebocoran UV daripada sumber lampu. Pemalar kadar purata pseudo kinetik tertib pertama untuk penguraian MB bagi 10 kali kitaran aplikasi berulang 90 min menggunakan lampu pendafluor dengan kebocoran UV

sebanyak 1.67, 4.35 dan 6.30 Wm^{-2} adalah masing-masing 0.0174 ± 0.0072 , 0.0381 ± 0.0039 dan $0.0577 \pm 0.0027 \text{ min}^{-1}$. Analisa menggunakan SEM-EDX, TGA dan FTIR menunjukkan berlakunya penguraian adunan polimer yang digunakan sebagai pelekat selepas digunasemula mengakibatkan penghasilan keperluan oksigen kimia (COD). Penguraian ENR-50 didapati berlaku lebih pantas berbanding penguraian PVC. Sebanyak 50 % daripada MB berkepekatan sebanyak 20 mg L^{-1} dimineralisasikan selepas rawatan pemfotomangkinan selama 4 jam menggunakan plat TiO_2 terpegun yang 'dibersihkan'. Tahap mineralisasi adalah selari dengan peratusan penguraian warna MB. Kehadiran komponen tak organik seperti SO_4^{2-} , NO_3^- , Cl^- dan perubahan pH dalam larutan terawat menunjukkan MB telah dimineralisasikan. TiO_2 yang dipegunkan pada penyokong polimer seperti PVC, akrilik dan PET kesemuanya menunjukkan aktiviti foto dalam penguraian larutan MB walaupun pada kadar yang lebih rendah. Secara keseluruhan, pemegungan serbuk TiO_2 melalui teknik penyaduran celup mudah ini adalah ringkas, berkesan, menjimatkan dan mempunyai kebolehlungan yang baik.

IMMOBILISATION OF TiO₂ POWDER ONTO GLASS PLATES VIA DIP-COATING TECHNIQUE USING ENR-50/PVC POLYMER BLEND AS ADHESIVES AND ITS PHOTOCATALYTIC APPLICATION

ABSTRACT

The objective of this work is to produce a reusable immobilised TiO₂ on glass plate utilizing polymer blend as adhesives for the photocatalytic degradation of methylene blue (MB) in aqueous solution. TiO₂ powder (99% anatase) was directly immobilised onto glass plates using epoxidised natural rubber (ENR-50)/ poly (vinyl) chloride (PVC) polymer blend as adhesives via simple dip-coating technique. The photocatalytic characterization of the immobilised TiO₂ powder was assessed using MB in aqueous solution as the model pollutant under the irradiation of 45W fluorescent lamp. The optimum ratio of ENR-50 to PVC for the immobilisation of TiO₂ was determined as 1:3. The photocatalytic efficiency of the immobilised TiO₂/ENR/PVC was better than the TiO₂ in slurry mode. The optimum catalyst loading was determined as 1.0 mg/cm² and the photocatalytic degradation rate of MB was highest at pH 12. The presence of aeration as oxygen source promoted the photocatalytic removal of MB. The photocatalytic degradation of MB was mainly governed by the UV residuals emanated from the 45 W fluorescent lamp. Reusability and reproducibility of the immobilised TiO₂/ENR/PVC improved proportionally with the intensity of UV irradiances from the light sources. The average pseudo first order rate constant of MB degradation for 10 cycles of 90 min repeated applications of the immobilised TiO₂ using light sources with UV irradiances of 1.67, 4.35 and 6.30 Wm⁻² were 0.0174 ± 0.00072 , 0.0381 ± 0.0039 and $0.0577 \pm 0.0027 \text{ min}^{-1}$, respectively. Subsequent analysis using SEM-EDX, TGA and FTIR revealed that the reliability of the immobilised TiO₂/ENR/PVC was however plagued by the

degradation of polymer blend used as adhesives upon recycled applications which resulted in the production of chemical oxygen demand (COD). The degradation of ENR-50 was faster than the elimination of PVC in the coating formulation. 50 % mineralization of 20 mg L⁻¹ MB was achieved after 4 hours of photocatalytic treatment using the 'cleaned' immobilised TiO₂. The degree of mineralization corresponded positively with the percentage of MB colour removal. The presence of inorganic compounds such as SO₄²⁻, NO₃⁻, Cl⁻ and the changes of pH in the treated solution represented the mineralized products of the model pollutants. The immobilised TiO₂/ENR/PVC on polymer supports such as PVC, acrylic and PET exhibited photo-activity in the degradation of MB albeit at lower degradation rate. Overall, the immobilization of TiO₂ powder via this technique is simple, effective, economical and reproducible.

CHAPTER 1

INTRODUCTION AND LITERATURE REVIEW

1.0 General

Basically, water pollution can be defined as the contamination of water bodies such as lake, sea, groundwater with various pollutants due to humans activities, which does not only endanger the inhabitants in these water bodies but also the consumers of the water. As of today, water pollution is a major global issue that needs to be addressed seriously, notably in fast developing countries. With the rapid growth of population as well as industries, it is inevitable that the demand for clean water also increases. Nevertheless, due to the escalating numbers of industrial and agricultural activities in most countries, effluents containing intolerable level of both organic and inorganic substances are being discharged into water bodies on a daily basis. Statistically, based on a report done by Malaysia's Department of Environment (DOE) in 2004, out of a record of 17,991 water pollution sources in Malaysia, 54% (8,414) of the sources originated from sewage treatment plant, 38 % (8,203) of the sources initiated from manufacturing industries and 3 % (504) came from agro-based industries [1]. Law enforcements and policy prescriptions on the management of industrial wastewater have long been executed extensively to combat water contamination but concurrently, efficient and cost effective water treatment technologies have to be adopted and developed in order to sustain cleaner water resources for the well-being of all.

Water treatment can be well described as the process of eliminating the presence of contaminants or decreasing the concentration of existing pollutants in water to an acceptable level for the purpose of desired end-use such as for industrial

processes and even as drinking water. Accordingly, an ideal water treatment system should be able to totally mineralize contaminants in polluted water without leaving behind any harmful intermediates or by products. Apart from that, the process should be economically sustainable and possibly, time-saving. Due to the recalcitrant nature of most pollutants, many existing water treatment methods have yet to attain this ideal condition.

Physical-chemical treatments such as coagulation, adsorption, membrane processes and reverse osmosis methods have been employed to a varying extent of effectiveness in removing pollutants from water. Nonetheless, these methods are non-destructive since they merely operate by transferring the pollutant from one phase to another phase or initiate secondary pollution by concentrating the contaminants [2]. This can lead to possible problems since many environmental enforcement agencies may classify the used sludge or adsorbents as harmful materials which require post-treatment. Further treatment of these solid wastes is often considered expensive and sophisticated. On the other hand, destructive wastewater treatment methods such as biological treatment, in both anaerobic and aerobic conditions, have proven to be effective but the presence of toxic organic contaminants can stifle the development of the active microorganisms the consequence of which inevitably reduces their degradation efficiency [3]. The maintenance of these bacteria can also be very costly and complicated. In appropriate situations, the destruction of organic pollutants and solid wastes can also be carried out via incineration but this may lead to the production of hazardous organics such as dioxins and furans [4]. Subsequently, these drawbacks have prompted intensive works on novel water treatment technologies which possess better efficiency and

consume fewer resources. This leads to the study of advanced oxidation processes (AOPs), a water cleaning technology which typically involved the formation of very powerful oxidizing radicals that leads to highly effective oxidation processes.

1.1 Advanced Oxidation Processes (AOPs)

AOPs can be generally defined as one type of water treatment technology that mainly involves the generation of very powerful oxidizing radicals (normally hydroxyl radicals with standard reduction potential, $E^\circ = 2.80\text{V}$ vs. SHE) which can unselectively initiate oxidative dissociation of organics or under certain circumstances, inorganic contaminants in aqueous effluents. Hydroxyl radicals are the most powerful oxidizing species after fluorine which possesses $E^\circ = 3.03$ vs. SHE. Contrary to other conventional water treatment method such as adsorption processes, AOPs are capable of converting hazardous materials in wastewater effluents into water and carbon dioxide, or otherwise, into other innocuous by-products. Furthermore, these ‘destructive’ chemical oxidative processes are able to mineralize wide range of contaminants and this has, in particular prevented the accretion of end-products. Major types of AOPs include the employment of ultra-violet (UV) light, hydrogen peroxide (H_2O_2), ozone (O_3), vacuum (V) and semiconductors such as titanium dioxide (TiO_2) [5]. Major AOPs can be summarized as shown in Figure 1.1.

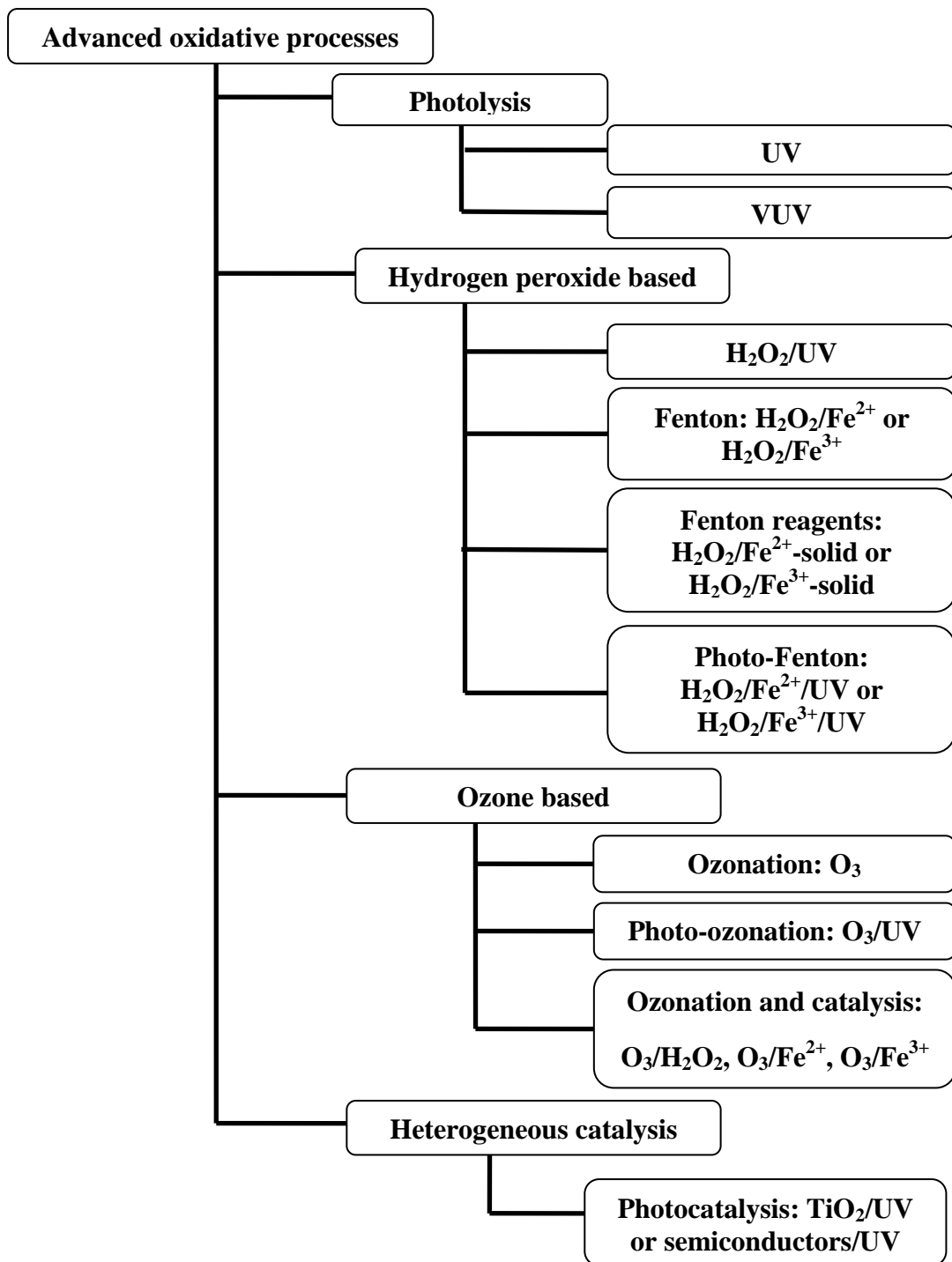


Figure 1.1: Major advanced oxidative processes (AOPs) processes and their various systems [5]

1.1.1 Processes of AOPs

Direct photolysis involves the interaction of UV light with pollutants in water to bring about their dissociation into intermediates which are eventually transformed to harmless by-products in the presence of light. In this process, the organic pollutants undergo absorption of UV light whereby its high energy radiation can result in the breakdown of chemical bonds and consequently, destruction of the organic compounds. Direct photolysis is deemed insufficient and inefficient for the degradation of persistent pollutants such as chlorinated and nitrated aromatics in water [6, 7]. The energy of UV light solely is inadequate to breakdown the chemical bonds of some organic species thus some contaminants are not degraded rapidly or effectively. This was confirmed by comparative studies which had also shown that the practice of direct UV photolysis in degradation of contaminants, namely chlorophenols, azo dyes, diuron and monocrotophos appeared to be less effective compared to other AOPs where irradiation was combined with hydrogen peroxide or ozone, and when homogeneous or heterogeneous catalysis was utilized [8 – 11]. The combination of notably short wavelength UV light with highly reactive chemical species such as hydrogen peroxide and ozone increases the degradation rate by multiple times due to the synergistic effect of efficient generation of hydroxyl radicals and the photon energy from the light.

During the UV based AOPs, organic contaminants are decomposed in two ways. The first way involves the direct photolysis of organic pollutants as mentioned earlier. The addition of H_2O_2 to the process initiates the AOPs conditions by generating $OH\cdot$ radicals. This often increases the destruction rate of pollutants considerably. In another route, H_2O_2 undergoes UV photolysis and a series of

propagation as well as termination reactions to produce $\text{OH}\cdot$ radicals. Subsequently, the generated $\text{OH}\cdot$ radicals will destroy the contaminants via $\text{OH}\cdot$ radical oxidation. Formation of $\text{OH}\cdot$ radicals in this process, therefore, determines the degree of pollutants removal. Hence, large dosages of H_2O_2 and long exposure of UV light are required in order to sustain the efficiency of this decontamination method. Another H_2O_2 induced AOPs involves the utilization of Fenton reagents to produce $\text{OH}\cdot$ radicals by means of addition of H_2O_2 to Fe^{2+} ions as catalyst. Simultaneously, this also generate Fe^{3+} ions due to the oxidation of Fe^{2+} ions. This process works on the fact that the iron catalyst is very easily acquired and it is a non toxic material. However, this process does not operate on the basis of the sole oxidation reaction only since the adoption of suitable pH value (2.7-2.8) can further catalyzed this reaction by initiating the reduction of Fe^{3+} in order to regenerate Fe^{2+} . The overall reaction is known as the Fenton process. Given that this reversible mechanism occurs at appropriate rate, the decomposition of pollutant via this method can be a sustainable process [12]. Photo assisted Fenton process is an extension of the Fenton process which manipulates the presence of UV light to cause photolysis of Fe^{3+} complexes to allow the reformation of Fe^{2+} . Decontamination of pollutants via H_2O_2 based AOPs however suffers from several drawbacks, namely the usages of expensive reactants such as H_2O_2 , the requirement of rigid controlled pH values and the generation of sludge which creates disposal problem.

Another type of AOPs which generates $\text{OH}\cdot$ radicals is known as ozonation. This is an oxidation process which the applications have also been tested with the combination of UV light and/or H_2O_2 . During ozonation, the dissolved organic contaminants are oxidized directly by O_3 which is a powerful oxidant itself. This is

due to the study that the decomposition of ozone in aqueous solution occurs through the generation of $\text{OH}\cdot$, which consecutively oxidize the pollutants. Evidently, when H_2O_2 is added to the ozonation process, the breakdown of O_3 is accelerated with the presence of more $\text{OH}\cdot$ radicals. Furthermore, the adoption of UV light into $\text{O}_3/\text{H}_2\text{O}_2$ system could improve the decontamination rate via photochemical generation of $\text{OH}\cdot$ radicals. However, this AOPs process is plagued with the low solubility of O_3 in water and the need of strict pH control since the O_3 decomposition mechanism involves the use of conjugated base [5].

Heterogeneous photocatalysis is another constituent of AOPs which has been studied extensively to decompose refractory compounds in wastewater effluents. This process is a photo-induced reaction that is based on the photocatalytic ability of a semiconductor to produce electron-hole pairs under irradiation which generates free radicals, namely hydroxyl radicals in order to initiate secondary reactions to remove the pollutants. Some of the semiconductors which are normally applied as photocatalyst are TiO_2 , ZnO and CdS [2, 6].

1.1.2 Environmental applications of AOPs

In conjunction with insufficient treatment brought by conventional and biological water purification methods, many AOPs induced studies have been carried out in the search of more sustainable water treatment technologies [8 - 10]. AOPs, despite their different pathways of processes, are merged by one similarity which is the presence of the highly reactive species such as the hydroxyl radicals in their overall mechanisms. These reactive radicals would lead to oxidative decompositions

of recalcitrant and non-biodegradable contaminants to harmless by-products or inert end products.

Over the years, apart from the research and development of water and wastewater treatment technologies, AOPs have also initiated other environmental applications such as soil treatment [13], groundwater remediation [14], conditioning of solid sludge [15] as well as treatments of volatile and semi volatile organic compounds [16, 17]. Environmental applications of AOPs on water and wastewater treatment have already been studied on wastewater effluents originated from diverse industries, namely textiles, pharmaceuticals, electronics, cosmetics, plastics, pesticides and so on which contain perilous and less biodegradable compounds such as cyanides, phenols, antibiotics, xenobiotics, ketones, chlorinated compounds, alcohols, aromatic compounds and acetates [18 - 22].

By considering the degree of pollution in effluents and the targeted treatments, AOPs can be applied solely or as feasible supports to the traditional biological and physicochemical treatments methods via combined processes. The combined processes practically offers better treatment results as compared to individual processes due to the synergistic or coupling effect permits by respective methods. Subsequently, AOPs can be engaged either at the pre-treatment stage, in which initial contaminants are converted into biodegradable intermediates ready for biological or physical treatments or at post-treatment level, whereby the ecological content of the pollutants are first removed and/or degraded before being treated by AOPs. As such, investigations on the application of Fenton oxidation process followed by aerobic biological treatment for the remediation of wastewater

containing recalcitrant and persistent compounds such as azo dyes have been documented [23 - 25]. Alternatively, pre-treatment of wastewater from paper industry by customary coagulation-flocculation methods as a preparatory step for subsequent treatment via heterogeneous photocatalysis has been reported [26].

However, amidst various AOPs processes, heterogeneous photocatalysis appears to be more effective and popular due to several advantages. The main advantages of heterogeneous photocatalysis are as the following:

- i. Semiconductors for the applications of photocatalysis are easily acquired and relatively inexpensive.
- ii. Most of the photocatalysts, especially TiO_2 (anatase) required for this technique are chemically and biologically stable.
- iii. Photocatalysts are reusable and many on-going studies are conducted to improve the reproducibility of the catalyst for long term use.
- iv. Oxidation processes under heterogeneous photocatalysis are capable of mineralizing wide ranges of persistent pollutants unselectively.
- v. Supplementary of expensive oxidants are redundant in this method because atmospheric oxygen from air pump is sufficient to be utilized as oxidant.
- vi. This process produces environmental friendly final products or by-products such as CO_2 and H_2O or other mineralized acids.
- vii. Water treatment via this method can be operated under the illumination of solar light as the photocatalyst can be stimulated under low energy light sources.

- viii. Under heterogeneous photocatalysis, oxidation and reduction can occur simultaneously, and therefore this process does not only have the ability to initiate reactions for the initial pollutants but also has large capabilities in purifying intermediates or by-products which are generated by the process.

1.2 Heterogeneous photocatalysis

1.2.1 Overview

While the subject of heterogeneous photocatalysis for both fundamental and applied perspectives has been immensely investigated, the definition of heterogeneous photocatalysis is still relatively ambiguous due to its rather complicated mechanism and diverse processes. As stated in an article by Herrmann [27], heterogeneous photocatalysis covers a large variety of reactions, namely oxidation, dehydrogenation, hydrogen transfer, isotopic exchange, metal deposition, water remediation, gaseous pollutant control and so on. Heterogeneous photocatalysis has found itself as an emerging AOP for environmental cleanups applications, especially when this fascinating process can be accomplished in various phases such as aqueous solution, pure organic liquid and even in gaseous state.

Similar to the established heterogeneous catalysis, this process mainly engages the migration of reactants in a liquid or a gaseous phase to the surface of the photocatalyst, followed by the adsorption of one or more of the reactants onto the surface and reactions at the adsorbed phase. Subsequently, this process persists on with the desorptions of the reactants and/or products of the reactions and finally, the elimination of products from the interface. The only dissimilarity that separates

heterogeneous photocatalysis from the other conventional catalytic processes is the photocatalytic reaction at the adsorbed stage. The catalyst or rather the photocatalyst in heterogeneous photocatalysis is stimulated via light energy instead of hydro or thermal energy at this stage. The photo activation process only takes place at the adsorbed phase although photoadsorption and photodesorption of reactants may possibly occur [27].

1.2.2 Background

The birth of heterogeneous photocatalysis three decades ago was provoked by Fujishima and Honda's 1972 discovery of photo-induced water splitting on TiO₂ electrodes. Back in late 1960s, the water splitting study was executed with a small electrochemical system in which an n-type TiO₂ semiconductor (rutile) was connected to a platinum black counter electrode through an electrical load. Upon the illumination of the TiO₂ electrode to near UV light ($\lambda < 415$ nm), electrons flowed from TiO₂ electrode to the platinum counter electrode through the external circuit, revealing that an oxidation reaction (oxygen gas evolution) has occurred at the TiO₂ electrode and a reduction reaction (hydrogen gas evolution) has taken place at the platinum electrode. This finding simply proved that water decomposition into oxygen and hydrogen may be possible under the presence of UV-visible light without the application of external electrical supply [28].

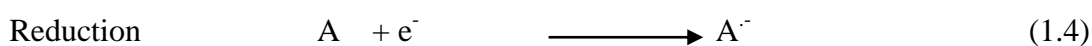
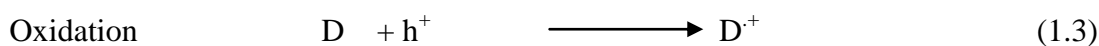
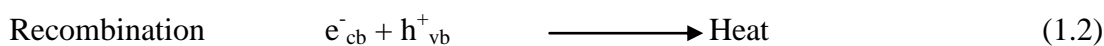
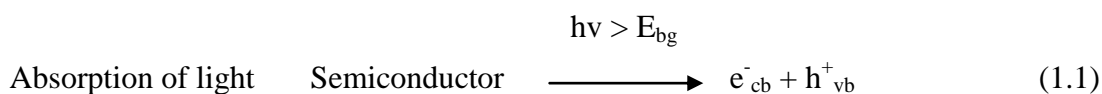
Since then, extensive studies had been initiated on the utilization of solar irradiation for the production of hydrogen as fuel source from water. Later, the water splitting study was further investigated without the use of external circuit and this marked the beginning of the phenomenal process by the name of heterogeneous

photocatalysis. Some years later in 1977, researchers Frank and Bard began to examine the possibilities of governing the redox reactions initiated by the illuminated semiconductor TiO_2 for the decomposition of cyanide in water and this has prompted many intensive works on the environmental purposes of heterogeneous photocatalysis until today [29].

1.2.3. Semiconductor mediated heterogeneous photocatalysis

As suggested by its term, ‘photocatalysis’, this process refers to the chemical transformation reactions initiated by the presence of light energy and catalyst. The catalysts required in this process correspond to semiconductors which are responsive to illuminations of light. Such reactions are due to the particular changes in the monomeric numbers N in the electronic structure of a semiconductor from atomic orbital to clusters. The band electronic structure of a semiconductor consists of the highest filled band (the valence band) and the lowest unfilled band (the conduction band) which are separated by a band gap, E_{bg} , a region depicting energy level in a perfect crystallite form and is normally valued in unit of electronvolts, eV. For the purpose of photo-induced reactions, the activation of a semiconductor photocatalyst can be achieved via the absorption of a photon of ultra-band gap energy, resulting in the transition of an electron, e^- from the valence band to the conduction band with the simultaneous generation of hole, h^+ in the valence band. The photo-generated electron-hole pairs are mainly involved in two processes, namely the reactions with electron donor or acceptors via different interfacial processes and major inhibition process concerning the recombination of electrons and holes. For a semiconductor to be efficient, these two mentioned processes must compete with one another

effectively [30]. These processes can be represented in Equations 1.1, 1.2, 1.3 and 1.4 [31]:



As illustrated in Figure 1.2, the valence and conduction band positions of various semiconductors are different. The reactivity of a photo-induced process is very much dependant on the valence and conduction band positions. Therefore, in an oxidation photocatalytic reaction, the redox potential of the photo-generated valence band hole must be adequately positive to generate the highly oxidizing radicals, hydroxyl radicals for the oxidation of pollutants to occur. On the other hand, for a semiconductor to perform as a photocatalyst in a reduction reaction, the redox potential of the photo-generated conduction band must be negative enough to initiate the reduction of molecular oxygen into superoxide. The production of electron-hole pairs are governed by the intensity and the photon energy of the light source used for the activation of a semiconductor.

According to Taghizadeh *et al.* [32], photochemical induced process concerning semiconductors can be divided into two significant categories: (i) the formation of highly reactive radicals resulted from the oxidation of hydroxide ions and reduction of oxygen which would initiate reactions with the pre-adsorbed

substrates at the solution interface and (ii) direct oxidation or reduction of the compounds that diffuse from the batch solution to the semiconductor particle surface.

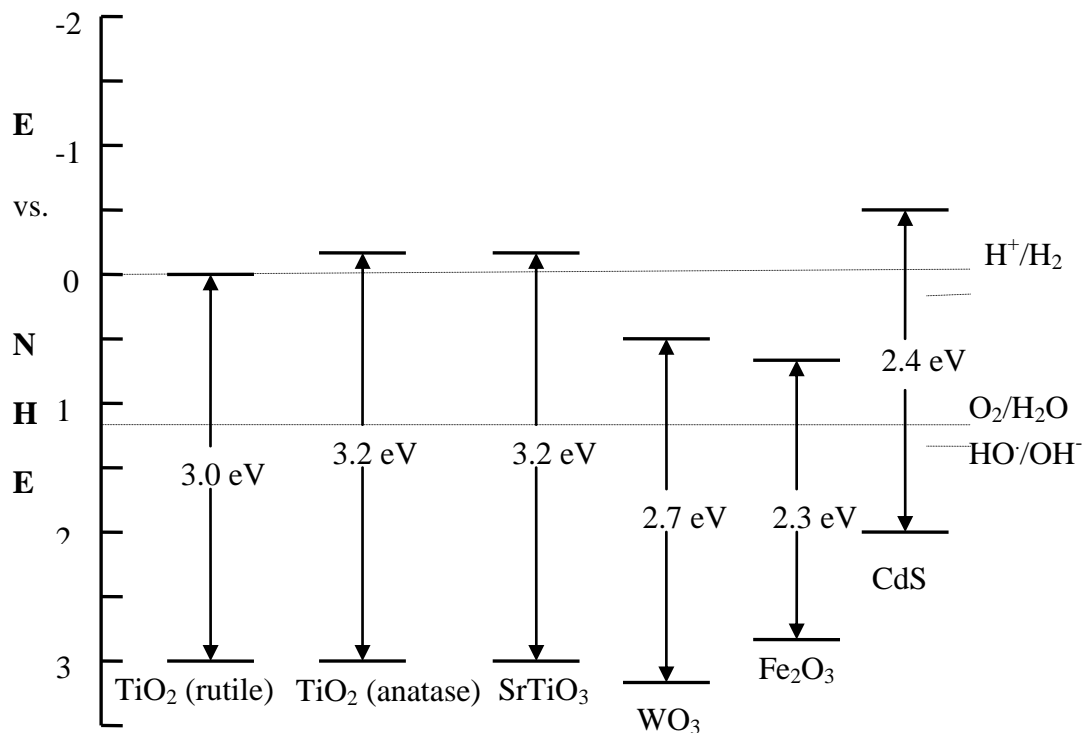


Figure 1.2: Valence and conduction band positions of some the most commonly used semiconductor photocatalysts at pH = 0 [30].

Similarly, in environmental applications, semiconductor photocatalysis essentially involves the irradiation of semiconductors with photon of energies greater than the band-gap energy in order to excite electrons from the valence band to the conduction band, leaving behind the positive holes. The positive valence band gradually generates hydroxyl radicals whereas the negative conduction band initiates the reduction of molecular oxygen or metal ions, which often serves as the oxidizing agent. Hence, the formation of highly oxidizing agents such as hydroxyl and superoxide radicals would attack the contaminants at or near the surface of the

semiconductor photocatalysts, resulting in the detoxification of pollutants via concurrent redox reactions [33]. In photocatalytic water remediation, oxidation reactions are applied to mineralize dissolved organic substances whereas reduction reactions are utilized for the removal of inorganic compounds such as heavy metal ions.

Some of the commercially acquired semiconductors that have been actively researched in photocatalytic studies for environmental cleanup are TiO₂ [29, 34], ZnO [35, 36], ZnS [37], Fe₂O₃ [38], WO₃ [39], CdS [40] and ZrO₂ [41]. In some works, two or more semiconductors are combined and modified with the aim of enhancing the photo-induced reactions [42-44] for better removal of pollutants. Despite of the many other semiconductors, most of the photocatalytic studies are dominated by the application of TiO₂ as the photocatalyst.

1.3 Titanium dioxide (TiO₂)

1.3.1 General

A member of the first transition series metals, titanium has the electronic structure of $3d^24s^2$. Discovered in 1791 in England by Reverend William Gregor who recognised the new element in ilmenite, titanium is the world's fourth most abundant metal after aluminium, iron and magnesium and the ninth most abundant element comprising about 0.63 % of the earth's crust. Ilmenite is one of the main ores for titanium and is widely used as a source of titanium metal. Several years later, titanium was rediscovered by a German chemist by the name of Martin Heinrich Klaporth who named the element after the Titans of the Greek mythology. Titanium metal is usually found bounded to other elements in nature. The element occurs

primarily in minerals, especially rutile, ilmenite and leucosene, and can also be found in rocks, coal, ash, soils and even in human bodies. Titanium commonly appears as impure compounds found in minerals in the form of TiO_2 , in which rutile constitutes 93 % to 96 % of TiO_2 , ilmenite contains 44 % to 70% of TiO_2 and leucosene may comprise up to 90 % of TiO_2 . Titanium can also appear in the form of titanium tetrachloride (TiCl_4) [45].

A metallic element, titanium is usually recognised for its high strength to weight ratio and its excellent resistance to corrossions. Titanium is also a strong metal which has low density and is relatively flexible. The melting point of titanium is 1668 °C and chemically, titanium is one of the few elements exist that burns in pure nitrogen gas at 800 °C to form titanium nitride. It is also able to withstand the attack of diluted acids and bases. Titanium dissolves in hot HCl giving Ti (III) chloro complexes and in HF or HNO_3 and HF to form fluoro complexes. Heated in HNO_3 will result in the formation of hydrous oxide [46].

It is estimated that approximately 98 % of the world's titanium production is meant for the refinement into TiO_2 , the white permanent pigments, while only the remaining 2 % is used for making titanium metals, rods, fluxes and other products. Due to its two most beneficial features, its resistance to corrosion and strength to weight ratio, titanium is widely applied in chemical industries, aircraft and marine equipments and turbine engines [45].

Titanium dioxide, also known as titanium (IV) oxide or titania, belongs to the family of transition metal oxides. The mass production of TiO_2 began in early 20th

century when TiO_2 started substituting hazardous lead oxides as white pigments in paint. Since then, TiO_2 is utilized actively as white pigments in paint, paper and plastics industries, which make up the major sectors of TiO_2 usages [45]. The applications of TiO_2 as pigments have expanded over the years in some sectors such as textile, food, pharmaceuticals, cosmetics, leather and mixed oxides. Due to its high refractive index, TiO_2 has also found itself as anti-reflection coating in solar cells and in optical devices. Furthermore, TiO_2 is also applied as gas sensors, biomaterials, catalysts, additives, carrier for metal and metal oxides and dielectric materials [45].

On an industrial scale, TiO_2 may be synthesised by either using the sulphate or the chlorine process. Briefly, the sulphate process involves the transformation of ilmenite to metal sulphates after reactions with sulphate acids followed by appropriate steps of hydrolysis, filtration and calcinations according to the desired crystallite forms of TiO_2 . On the other hand, the chlorine process employs rutile, which is obtained from ilmenite via Becher process. In Becher process, iron oxide found in ilmenite is reduced to metallic iron and later is reoxidised to iron oxide, unravelling out the TiO_2 as synthetic rutile of 91-93 % purity. Later on, the produced rutile is reacted with chlorine to produce TiCl_4 , which is purified and reoxidized to yield highly pure TiO_2 . Even though both methods are applicable to produce TiO_2 , factors such as the accessibility of raw materials, waste management costs, transportation and environment are fairly put into consideration in deciding to use one method instead of the other [45].

1.3.2 Crystal structures of TiO₂

Titanium dioxide has three main polymorphs in nature, namely rutile (tetragonal), anatase (tetragonal) and brookite (orthorhombic). These three crystallite structures comprise of distorted octahedral (TiO₆²⁻) that are linked differently by vertices and edges. Anatase can be seen as a zigzag structure in which each octahedron shares four edges with the other four octahedral. As for rutile, two octahedral edges are shared to build linear chains along the direction of 001 plane and the octahedral chains that are connected to one another via vertices shared bonding electrons. In brookite, each octahedron shares three edges and the octahedrals assembly leads to a crystalline structure with tunnels along the *c*-axis [47]. The three crystal structures of TiO₂ are illustrated in Figure 1.3 and their physical properties are summarized in Table 1.1.

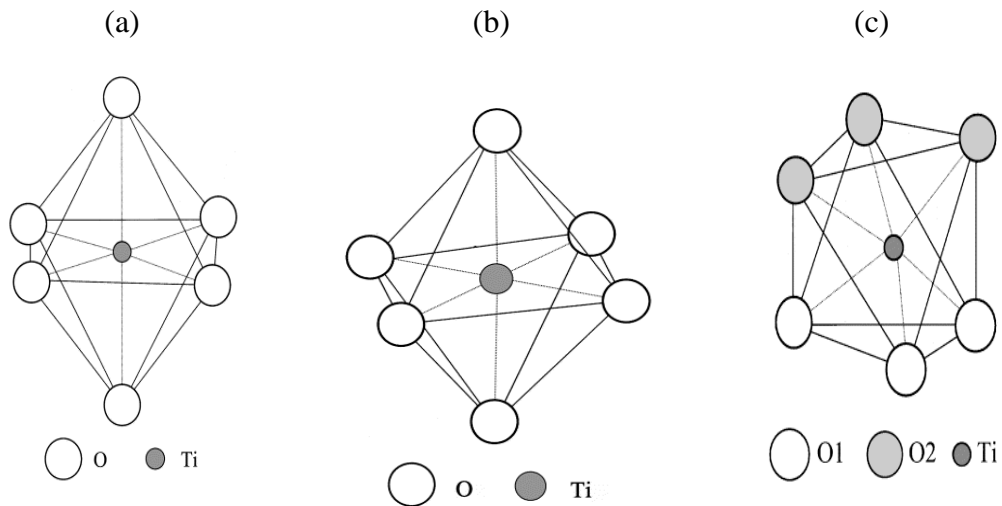


Figure 1.3: The representative crystals structures of (a) anatase, (b) rutile and (c) brookite [48].

Based on thermodynamic calculations, rutile is the most stable of all three crystalline forms of TiO₂ at all temperature and pressure up to 60 Kbar. Anatase and brookite are metastable and are prone to transformation when heated. However, the

slight discrepancy in Gibbs free energy (4-20 KJ/mole) among these three phases shows that anatase and brookite are just as stable as rutile at ambient temperature and pressure [45].

The conversion of anatase to rutile has been studied for mechanical as well as application purposes, especially in photocatalytic driven field, whereby the phase of TiO_2 play a major role in determining the reactivity of the process. At room temperature, anatase is kinetically stable and the phase transition of anatase to rutile occurs during calcinations from 600 °C to 1100 °C. The transformation of anatase to rutile is basically due to the increase in pressures and temperatures, in which these two factors are governed by primary particle size as well as the methods, used during preparation [49].

Anatase and rutile phases have been studied most extensively in photocatalytic induced activity whereas another phase of TiO_2 , brookite is difficult to prepare and amorphous TiO_2 is not reactive towards light energy [49]. In most photocatalytic studies, however, anatase phase is preferred over the rutile phase because anatase exhibits better electron mobility, lower dielectric constant, less dense and lower deposition temperature which allows the applications of low thermally resistance materials as supports in its immobilisation process.

Table 1.1: Physical properties of anatase, rutile and brookite [45]

Form	Crystal	Space group	Lattice constants (nm)			
			<i>a</i>	<i>b</i>	<i>c</i>	<i>c/a</i>
Anatase	Tetragonal	D _{4h} ¹⁹ -I4 ₁ /amd	0.3733	-	0.937	2.51
Rutile	Tetragonal	D _{4h} ¹⁴ -P4 ₂ /mmm	0.4584	-	0.2953	0.644
Brookite	Orthorhombic	D _{2h} ¹⁵ -Pbca	0.5436	0.9166	-	0.944
Density (kg m ⁻³)		Band gap (eV)	Refractive index		<i>ng</i>	<i>np</i>
Anatase	3830	3.26			2.5688	2.6584
Rutile	4240	3.05			2.9467	2.6506
Brookite	4170				2.8090	2.677
Dielectric properties	Frequency (Hz)	Temperature (K)	Dielectric constant			
Rutile, perpendicular to optical <i>c</i> -axis	10 ⁸	290-295	86			
Rutile, parallel to optical <i>c</i> -axis	-	290-295	170			
Rutile, along <i>c</i> -axis	10 ⁷	303	100			
Anatase, average	10 ⁴	298	55			

1.4 TiO₂ as semiconductor photocatalyst

The application of semiconductor in photocatalysis for water and wastewater treatment technology has attracted attention globally. One of the most crucial factor in determining the effectiveness and efficiency of the pollutants treatment process is the choice of the semiconductor used as the photocatalyst in the treatment system.

The photo-activation of a semiconductor to generate electron-hole pairs for redox reactions is determined by the band gap energy between its valence band and its conduction band. Therefore, the band gap energy is basically used as a benchmark when choosing compatible semiconductors for photocatalytic studies. Table 1.2 depicts the band gap energies of some of the most used photocatalysts and their threshold wavelengths. Although semiconductors with lower band gap energy are

preferred for photocatalysis, especially when solar irradiation is applied, the utilization of semiconductor such as CdS is unfavourable as it is susceptible to photodecomposition. Subsequently, this leads to the leaching of cadmium, a specifically toxic metal itself, into the treated water [31].

Table 1.2: The band positions of some common semiconductors in aqueous solution at pH 1 [31].

Semiconductor	Band gap (eV)	Wavelength (nm)
TiO ₂	3.2	380
SnO ₂	3.9	318
ZnO	3.2	390
ZnS	3.7	336
WO ₂	2.8	443
CdSi ₂	2.5	491
CdSe	1.7	730
GaAS	1.4	887
GaP	2.3	540

Ideally, a semiconductor photocatalyst must be photoactive, biologically and chemically inert, applicable in visible and/or UV light region, stable towards light, able to unselectively degrade wide ranges of pollutants, easily acquired, easy to handle, inexpensive and does not pose risks or hazards to both environment and humans. Among the available semiconductors, TiO₂ satisfies most of the ideal criteria.

Solar irradiation which contains about 3-5 % UV of wavelength, $\lambda < 380$ nm can be used as a light source to activate TiO₂. The application of sunlight as a light source is encouraged as it is a renewable source of energy. Therefore, this has prompted many works on the modification of TiO₂ to respond to visible light (about 45 % of the solar spectrum) in order to achieve better photocatalytic efficiency under

sunlight [50]. Some of the modification approaches that have been taken are non-metals doping [51-52] and metal oxide mixing [43-44, 50]. Yang *et al.*, [51] synthesised carbon and nitrogen co-doped TiO₂ and found out that due to the increased surface area and optical shift governed by the dopants, the photocatalytic efficiency of the doped catalyst was enhanced as compared with pure TiO₂ under both visible light and UV exposure. In a study conducted by Pavasupree *et al.*, [50], TiO₂-CeO₂ nanopowders with limiting amount of 5 % mol of CeO₂ was produced using modified sol-gel processes and it was observed that the mixed metal oxides demonstrated 2-3 times better photocatalytic activity as compared with pure TiO₂ under visible light.

1.5 General mechanism pathway of TiO₂ photocatalysis

The common process of TiO₂ photocatalysis involves the excitation of an electron from the valence band to the conduction band when it is exposed with UV light ($\lambda < 380$ nm), leaving a hole in the valence band. Detailed mechanism of TiO₂ photocatalysis have been discussed in literatures [27, 34, 53] and summarized here [54]. As TiO₂ is irradiated with light energy of equal or more than its band gap energy (3.2 eV for anatase phase), electrons in conduction band (e^-_{CB}) and holes in valence band (h^+_{VB}) are produced according to Equation 1.5:



These photo generated species undergo charge transfers with adsorbate such as oxygen, hydroxyl ions or organic substrates on the surface of TiO₂. The charge transfer process is continuous and direct decomposition of the organic substrate is

possible. The trapping of the electrons at the conduction band by charge carriers is faster (100 ps) than the trapping of the hole (10 ns) [53]. The trapped holes react with the surrounding water molecules or hydroxyl ions, leading to the formation of highly reactive radicals, namely hydroxyl radical $\cdot\text{OH}$. The holes may also initiate direct oxidization of the contaminating species (R). These processes are shown in Equations 1.6, 1.7 and 1.8:



The excited electrons react with electron acceptors such as the oxygen adsorbed or dissolved in the water as represented in Equation 1.9:



It is believed that the hydroxyl radicals ($\cdot\text{OH}$) and superoxide radical anions ($\text{O}^{\cdot-}_2$) are the major oxidizing agents in the photocatalytic reactions [54-55]. Some other oxidizing species that may be produced are reported as H_2O_2 and HOO^\cdot [56]. Without the presence of electron acceptors and donors, there is also a possibility that the electrons and holes may recombine either on surface or in the bulk of TiO_2 , as shown in Equation 1.10:



These processes can be illustrated as in Figure 1.4.

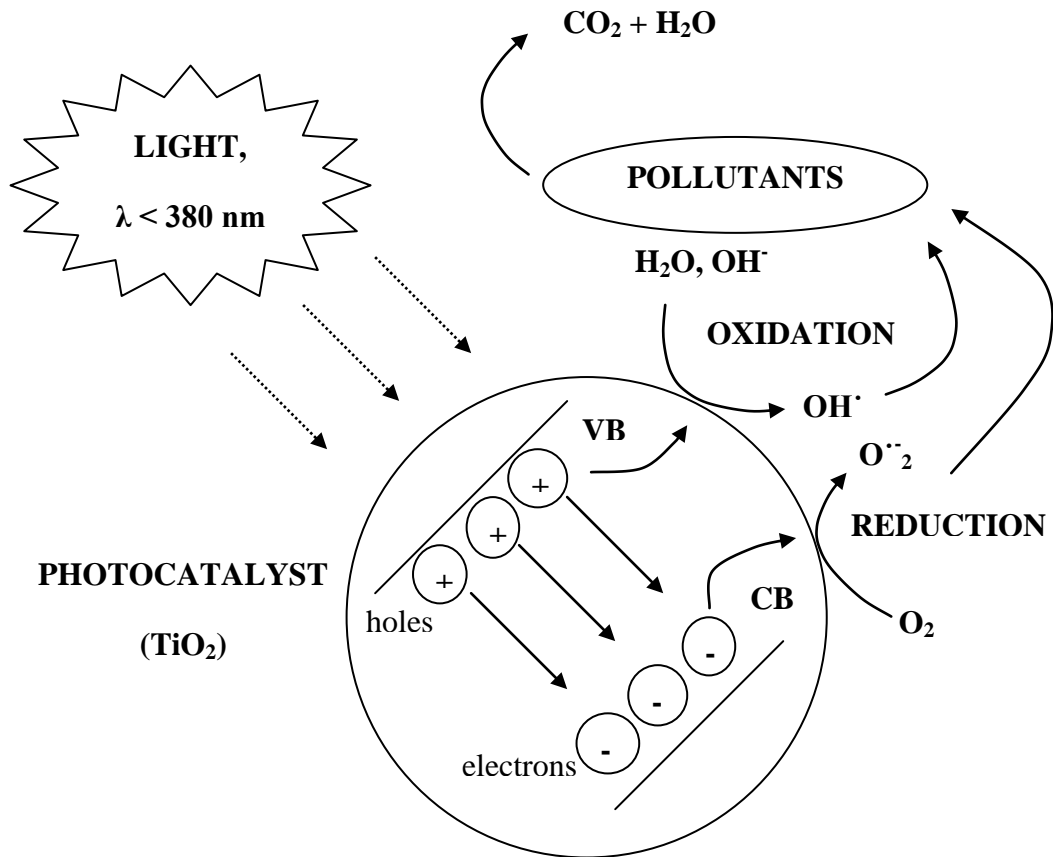


Figure 1.4: General mechanism pathway of TiO₂ photocatalysis [54].

1.6 Langmuir-Hinshelwood process

Direct photocatalytic reactions pathway discussed earlier in Section 1.5 can be well described as the Langmuir-Hinshelwood process. This process follows the formation of electrons and holes upon the photo excitation of a catalyst. As explained previously, the hole is trapped by the adsorbed substrates and subsequently generates highly reactive radicals. This reactive species then decays via two ways, namely recombination with the photo generated electrons or undergo chemical reactions,

yielding the product of the reactions. This process can be accessed and evaluated quantitatively using the Langmuir-Hinshelwood kinetic model [5].

Initially studied for the quantification of gaseous-solid reactions, the Langmuir-Hinshelwood kinetic model is presently used to describe the reactions between liquid and solids. Based on this kinetic model, the rate of the reaction corresponds linearly with the portion of surface (r) covered by the substrate (θ) as shown in the following Equation 1.11 (adapted from Valente *et al.*, [57]):

$$r = dC/dt = k\theta \quad (1.11)$$

Langmuir's model that ascertains adsorption on solid substrate can be described as in Equation 1.12. Therefore the previous Equation 1.11 becomes proportional to the Equation 1.13:

$$\theta = KC / (1+KC) \quad (1.12)$$

$$r = dC/dt = k\theta = kKC / (1+KC) \quad (1.13)$$

In Equation 1.13, k is the true rate constant which covers a number of operational parameters such as mass transfer, aeration rate and so on, whereas K is the constant of adsorption equilibrium in Langmuir-Hinshelwood. For photocatalytic studies, the value K is attained empirically through kinetic study in the presence of light and is better than that obtained during adsorption studies. C is the concentration of the substrate at time t .